

# The vacuolar kinase Yck3 maintains organelle fragmentation by regulating the HOPS tethering complex

Tracy J. LaGrassa and Christian Ungermann

Biochemie-Zentrum der Universität Heidelberg, 69120 Heidelberg, Germany

**T**he regulation of cellular membrane flux is poorly understood. Yeast respond to hypertonic stress by fragmentation of the normally large, low copy vacuole. We used this phenomenon as the basis for an *in vivo* screen to identify regulators of vacuole membrane dynamics. We report here that maintenance of the fragmented phenotype requires the vacuolar casein kinase I Yck3: when Yck3 is absent, salt-stressed vacuoles undergo fission, but reassemble in a SNARE-dependent manner, suggesting that vacuole fusion is disregulated. Accordingly, when Yck3 is deleted, *in vitro* vacuole fusion is increased,

and Yck3 overexpression blocks fusion. Morphological and functional studies show that Yck3 modulates the Rab/homotypic fusion and vacuole protein sorting complex (HOPS)-dependent tethering stage of vacuole fusion. Intriguingly, Yck3 mediates phosphorylation of the HOPS subunit Vps41, a bi-functional protein involved in both budding and fusion during vacuole biogenesis. Because Yck3 also promotes efficient vacuole inheritance, we propose that tethering complex phosphorylation is a part of a general, switch-like mechanism for driving changes in organelle architecture.

## Introduction

Homeostasis of eukaryotic cells is largely dependent on dynamic compartmentalization of the endomembrane system. Compartments are designed so that they can exchange materials and undergo dramatic morphological changes in order to meet the demands of metabolism, growth, and environment. Organelle architecture seems to be governed by the same processes that facilitate inter-compartmental exchange, namely, membrane fission and fusion (for reviews see Mellman and Warren, 2000; Bonifacino and Glick, 2004). Although the basic machineries of this so-called vesicular transport are well characterized, we understand less about the coordinated mechanisms that keep them under spatiotemporal control. This regulation is essential for normal and pathological pathways of organelle assembly and disassembly and, in fact, provides membrane transport with the context that results in a functional cell. Thus, the understanding of transport regulation is a primary focus for cell biology.

The lysosome-like vacuole of budding yeast *Saccharomyces cerevisiae* is a robust model for studying the cell biological aspects of regulated membrane flux. Several principles of vesicle targeting and membrane fusion have been established through genetic and cell biological studies of vacuole biogenesis and biochemical analysis of isolated vacuoles (Burd et al., 1998; Mullins and Bonifacino, 2001; Wickner, 2002). Vacuoles are particularly suitable for studying organelle architecture, because they are generally large, low copy, and regulate their morphology in response to many of the same signals that control morphogenesis of other organelles (Conibear and Stevens, 2002; Weisman, 2003). For example, vacuole inheritance is coordinated by the cell cycle. Early in G1, vesicular-tubular “segregation” structures bud from the vacuole and migrate from the mother cell into the emerging daughter, where they fuse to reform the characteristic low copy vacuole (for review see Weisman, 2003). Additionally, vacuoles are sensors for environmental stress. When yeast are placed into hypertonic medium, vacuoles undergo a rapid decrease in volume via a process involving phospholipid synthesis, in order to restore osmotic balance to the cell (Bone et al., 1998; Nass and Rao, 1999; Bonangelino et al., 2002b). Here, we will refer to this volume decrease as vacuole “fragmentation,” but it may actually be the result of a combination of fragmentation, tubulation, ruffling (crenellation), deflation, and retrograde transport.

Correspondence to Christian Ungermann: cu2@ix.urz.uni-heidelberg.de

Abbreviations used in this paper: ALP, alkaline phosphatase; CKI, casein kinase I; GAP, GTPase activating protein; GEF, guanine nucleotide exchange factor; HOPS, homotypic fusion and vacuole protein sorting complex; PIC, protease inhibitor cocktail; PS, 10 mM Pipes-KOH, pH 6.8, 200 mM sorbitol; PSK, PS with 150 mM KCl; PtdIns(3,5)P<sub>2</sub>, phosphatidylinositol 3,5-bisphosphate; wt, wild-type.

The online version of this article contains supplemental material.

Conversely, vacuole fusion represents an adaptation for hypo-osmotically-stressed cells, allowing cells to accommodate the influx of water by increasing the vacuole volume. Cell cycle-dependent inheritance and fission/fusion during osmotic stress are among several examples of situations in which vacuoles undergo regulated responses to changes in cell physiology (Weisman, 2003).

A number of components involved in vacuole fusion, fission, and inheritance have been identified (Wickner, 2002; Weisman, 2003). Despite these advances, we still do not understand how these antagonistic processes of organelle growth and disassembly are regulated. What signals induce vacuole segregation structures, fragmentation during salt stress, or vacuole growth after inheritance has been completed? To address these questions, we sought to characterize mutants with defects in vacuole morphology, beginning with those having enlarged (class D) vacuoles (Bonangelino et al., 2002a; Seeley et al., 2002). We screened these mutants for their ability to undergo regulated in vivo fragmentation during hypertonic stress, in an attempt to pinpoint the molecular cause for their lost morphological flexibility. Here, we found that failure to undergo fission is only one explanation for the class D vacuole phenotype. We report that negative regulation of fusion by the vacuolar casein kinase I (CKI) Yck3 is an additional mechanism for vacuole size control.

## Results

### A screen for mutants defective in the vacuolar response to hypertonic stress

We used the phenomenon of vacuole volume shrinkage during high salt stress as the basis for a limited screen of the haploid Euroscarf deletion library, focusing on mutants that have partial class D vacuole morphology (for stains see Tables I and II). As depicted in Fig. 1 A, cultures were grown to log phase, and vacuoles were labeled by pulse-chase with the lipophilic dye FM4-64, which follows the endocytic pathway to the vacuole membrane (Vida and Emr, 1995). Cells were then transferred to fresh medium containing 0.4 M NaCl, which is a salt concentration sufficient to drive fragmentation of wild-type (wt) vacuoles (Bonangelino et al., 2002b). After 10 or 60 min of growth under these conditions, vacuole morphology (Fig. 1 B) was visualized by fluorescence microscopy. The results of the screen are summarized in Table II (see Table S1 for a detailed analysis, available at <http://www.jcb.org/cgi/content/full/jcb.200407141/DC1>).

As expected, wt vacuoles became fragmented within a 10-min salt exposure, whereas *fab1Δ* vacuoles stayed large and round (Fig. S1, A and B, available at <http://www.jcb.org/cgi/content/full/jcb.200407141/DC1>). *Fab1* is a lipid kinase whose increased activity—the generation of phosphatidylinositol 3,5-bisphosphate (PtdIns[3,5]P<sub>2</sub>)—is necessary for vacuole fragmentation during hypertonic stress (for review see Weisman, 2003). Similarly, *vps3Δ* vacuoles failed to fragment (Fig. S1 C). The *VPS3* gene product plays a role in vacuole protein transport, and is required for vacuole inheritance (Raymond et al., 1990). The class D phenotypes of *vps3Δ* and *fab1Δ* might therefore be due to a fission defect.

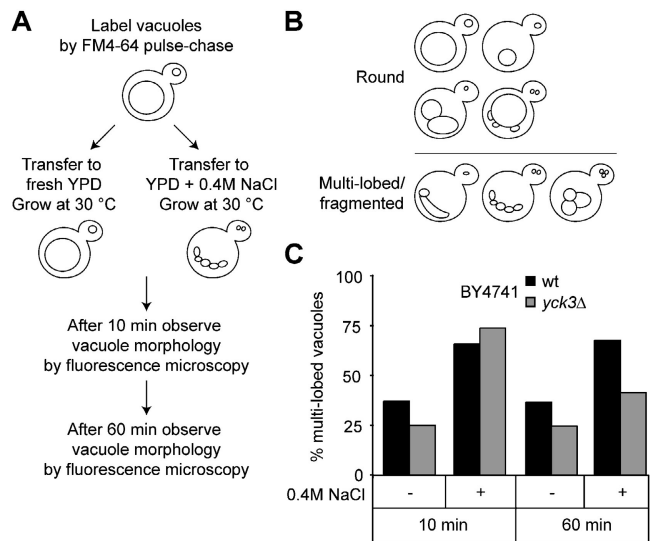


**Figure 1. Screen for vacuolar hypertonic stress response mutants.** (A) Schematic of the screen of in vivo vacuole morphology of salt-stressed deletion mutants. For hypertonic stress, cells were transferred to YPD containing 0.4 M NaCl, final. See Table II, Fig. S1, and Table S1 for a summary of results and quantification. (B) Observed vacuole morphologies and their classification. (C) Wt/*yck3Δ* vacuole morphology during prolonged salt stress. Comparison of vacuole morphology (% of cells containing multi-lobed vacuoles) for BY4741 wt and *yck3Δ* in the absence (–) or presence (+) of salt stress; cells were observed after 10 and 60 min. At least 450 cells were counted for each condition.

This, however, is not a satisfying explanation for the phenotype seen for other class D mutants; in most mutants, vacuoles became fragmented. Fragmentation was not dependent on the Hog1 MAPK pathway, the major mechanism for long-term adaptation to high osmolarity (Fig. S1 D; for review see Mager and Siderius, 2002). This is consistent with the finding that PtdIns(3,5)P<sub>2</sub> synthesis during hyper-osmotic stress is also independent of this pathway (Dove et al., 1997). Interestingly, we observed that vacuole fragmentation was maintained in the wt strain and most mutants, including the *hog1* deletion, during prolonged salt exposure (Table II; Fig. S1). This was unexpected because PtdIns(3,5)P<sub>2</sub> increases only transiently in the presence of 0.4 M NaCl (Dove et al., 1997). Prolonged vacuole fragmentation may thus require an apparatus beyond PtdIns(3,5)P<sub>2</sub>-directed fission, perhaps involving PtdIns(3,5)P<sub>2</sub> effectors and/or the active inhibition of vacuole fusion.

### Deletion of *yck3*, a CKI, causes a novel defect in vacuole morphology regulation

The *yck3Δ* mutant exhibited a unique stress response, which was consistent with a failure to down-regulate vacuole fusion (Table II; Fig. S1 E). After 10 min of salt stress, *yck3Δ* vacuoles achieved a level of vacuole fragmentation similar to wt, demonstrating that Yck3 is not an upstream regulator of the PtdIns(3,5)P<sub>2</sub>-related fission cascade. However, although wt vacuoles stayed small, *yck3Δ*'s became large again (Fig. 1 C; Fig. S1, A and E). We analyzed the same deletion in a strain that typically has a single, enlarged vacuole (BJ3505, one of the vacuole fusion reporter strains), and confirmed these observa-

Table I. Yeast strains used in this study

Strain	Genotype	Reference
ANY11-2c	MATa <i>rst2-1/hrr25-2 ura3 leu2 trp1 his3 his4</i>	Nakano lab collection
ANY21	MATa <i>ura3-52 leu2-3, 112 trp1-289 his3 his4 suc gal2</i>	Murakami et al., 1999
BJ3505	MATa <i>pep4Δ::HIS3 prb1-Δ1.6R HIS3 lys 2-208 trp1-Δ101 ura3-52 gal2 can</i>	Haas, 1995
BY4741	MATa <i>his3Δ1 leu2Δ0 met15Δ0 ura3Δ0</i>	Brachmann et al., 1998
CUY122	BJ3505; <i>ypt7Δ</i>	Haas et al., 1995
CUY345	BJ2168; <i>pYES2-GAL10pr-GYP7(359-745)-HIS6</i>	Eitzen et al., 2000
CUY399	BJ3505; <i>vps41Δ::KANMX4</i>	This study
CUY425	BJ3505; <i>TRP1::VPS41-6HA</i>	This study
CUY548	BY4741 <i>yck3Δ; pep4Δ::URA3</i>	This study
CUY551	BY4741 <i>yck3Δ; pho8Δ::URA3</i>	This study
CUY575	CUY399 [BJ3505 <i>vps41Δ</i> ]; <i>pRS406.NOP1pr-GFP-VPS41</i>	This study
CUY591	BY4741 <i>pho8Δ; pRS406.NOP1pr-GFP-VPS41</i>	This study
CUY592	BY4741 <i>yck3Δ; pRS406.NOP1pr-GFP-VPS41</i>	This study
CUY628	BY4741 <i>yck3Δ; pRS415.NOP1pr-GFP-VPS41</i>	This study
CUY654	BY4741 <i>pho8Δ; pCUP1pr-VAC8-GFP</i>	This study
CUY655	BY4741 <i>yck3Δ; pCUP1pr-VAC8-GFP</i>	This study
CUY785	BJ3505; <i>yck3Δ::KANMX4</i>	This study
CUY798	BY4741; <i>HIS5::PHO5pr-GFP-MYC-YCK3</i>	This study
CUY804	CUY548 [BY4741 <i>pep4Δyck3Δ</i> ]; <i>vps41Δ::LEU2</i>	This study
CUY820	BY4741; <i>HIS5::PHO5pr-GFP-MYC-YPT7</i>	This study
CUY822	BY4741 <i>yck3Δ; HIS5::PHO5pr-GFP-MYC-YPT7</i>	This study
CUY887	BY4741; <i>pRS415.NOP1pr-GFP-VPS41</i>	This study
CUY954	BY4741 <i>vac8Δ; yck3Δ::URA3</i>	This study
CUY955	BY4741 <i>pep4Δ; HIS3MX6::GALpr-YCK3</i>	This study
CUY956	BY4741 <i>pho8Δ; HIS3MX6::GALpr-YCK3</i>	This study
CUY959	BY4741; <i>HIS5::PHO5pr-GFP-MYC-PHO8</i>	This study
CUY960	BY4741 <i>yck3Δ; HIS5::PHO5pr-GFP-MYC-PHO8</i>	This study
CUY961	BY4741; <i>HIS5::PHO5pr-GFP-MYC-VAM3</i>	This study
CUY979	BY4741 <i>yck3Δ; HIS5::PHO5pr-GFP-MYC-VAM3</i>	This study
CUY985	CUY122 [BJ3505 <i>ypt7Δ</i> ]; <i>yck3Δ::KANMX4</i>	This study
Mat-A deletion library strains	BY4741; <i>ORFΔ<sup>a</sup> ::kanMX4</i>	Dujon, 1998

<sup>a</sup>Strains used from deletion library are *pho8Δ*, *pep4Δ*, *yck3Δ*, and others shown in Tables II and III.

tions (Fig. 2, A and B). If deletion of *yck3* results in failure to down-regulate vacuole fusion during hypertonic stress, introduction of an additional mutation that blocks vacuole fusion should revert this phenotype. *Nyv1* is a vacuolar R-SNARE that seems to function exclusively in homotypic vacuole fusion (Fischer von Mollard and Stevens, 1999). Its deletion, however, does not disturb vacuole morphology, leading to the suggestion that *Nyv1* can be replaced by other SNAREs in vivo (Thorngren et al., 2004). To address these issues, we constructed an *nyv1Δ yck3Δ* double deletion. *Nyv1Δ* vacuoles, as well as *nyv1Δ yck3Δ* vacuoles, became dramatically fragmented during hypertonic stress and stayed that way (Fig. 2, C and D). This indicates that *Nyv1* is required for fusion of *yck3Δ* vacuoles in vivo.

*YCK3/CKI3* encodes one of four budding yeast CKI isoforms (X. Wang et al., 1996). CKI family kinases are abundant, conserved, and multifunctional. Several studies have implicated them in vesicular transport in metazoans and yeast (X. Wang et al., 1996; Panek et al., 1997; Murakami et al., 1999; for review see Gross and Anderson, 1998), but a general mechanism for their action has been elusive. *Yck3* has no known in vivo substrates and, apart from its localization to vacuoles via the adaptor protein (AP)-3-dependent route (Sun et al., 2004), is a mystery.

### Yck3 influences the tethering stage of in vitro vacuole fusion

These results (and *Yck3*'s vacuolar enrichment; Fig. 3 A, 6D; Sun et al., 2004) led us to hypothesize that *Yck3* is a negative regulator of in vivo vacuole fusion during hypertonic stress. To address this possibility, we isolated *yck3Δ* vacuoles, and used a quantitative content mixing assay (Haas, 1995) to analyze their fusion in vitro. *Yck3Δ* vacuoles fused, on average, 40% better than the cognate wt vacuoles (Fig. 3 C). This result did not appear to be due to an increase in vacuole fusion machinery or assay reporter protein (Fig. 3, E and F; Fig. 7), and a *yck3Δ* vacuole size increase was observed with an independent visual fusion assay (Fig. S2, A and B, available at <http://www.jcb.org/cgi/content/full/jcb.200407141/DC1>).

If *Yck3* is a negative regulator of vacuole fusion, then vacuoles containing excess *Yck3* should fuse poorly. Indeed, overproduction of *YCK3* (*GAL-YCK3*) caused a 75% reduction in in vitro vacuole fusion, even when fusion was stimulated with recombinant *Sec18* (Fig. 3 D). These vacuoles have near wt levels of *Pho8* reporter protein and vacuole markers (Fig. 3, E–G; Fig. 6 D), but do appear to have other defects in vacuole biogenesis: whereas growth in galactose causes wt vacuoles to become fragmented in vivo, *GAL-YCK3* vacuoles are large and

Table II. Screen for vacuole response to hypertonic stress

vacuole morphology <sup>a</sup> : 10' YPD, 10' YPD + 0.4 M NaCl, 60' YPD + 0.4 M NaCl					
					
<b>Class D</b>	<i>wt</i>	<i>fab1</i>	<i>rom2</i>	<i>yck3</i>	<i>ies6?</i>
	<i>arc18<sup>b</sup></i>	<i>gon7<sup>c</sup></i>			<i>gon7?</i>
	<i>bem2</i>	<i>ies6<sup>c</sup></i>			
	<i>bub1</i>	<i>vps3</i>			
	<i>cka2</i>	<i>vps15<sup>c</sup></i>			
	<i>BJ nyv1<sup>d</sup></i>				
	<i>vma5</i>				
	<i>vps8</i>				
	<i>vtc1</i>				
<b>Hyperosmotic stress</b>	<i>hog1</i>				
	<i>rck2</i>				
<b>Other</b>	<i>ymr291w</i>				<i>vac8</i>
	<i>hrr25-2<sup>e</sup></i>				(class B)

For experimental data, see Table S1.

<sup>a</sup>The vacuole phenotypes observed for each of the three conditions are indicated by the cartoon.

<sup>b</sup>Deletions in BY4741, thus compared to BY4741 wt.

<sup>c</sup>It was unclear whether *ies6Δ*, *gon7Δ*, or *vps15Δ* had predominantly class D or class B phenotypes; they were ~60% fragmented under all conditions.

<sup>d</sup>Deletion in the BJ3505 strain, thus compared to BJ3505 wt.

<sup>e</sup>Mutation of the CKI isoform *HRR25* in the ANY21 strain (ANY11-2c), thus compared to ANY21.

FM4-64 localization is dispersed, indicating a delay in endosome-to-vacuole transport (Fig. S2 D).

In vitro vacuole fusion is divisible into several assayable stages (priming, docking, and content mixing), making it possible to determine the step in which a particular mutant is impaired (for review see Wickner, 2002). During priming, SNAREs and tethering proteins in a “cis-complex” are disassembled in an ATP- and Sec18/17 (yeast NSF/α-SNAP)-dependent manner. Functionality of this stage is signaled by Sec17 release from the vacuole (Mayer et al., 1996). Sec17 release from both GAL-*YCK3* and *yck3Δ* vacuoles was comparable to wt, indicating that Yck3 does not affect the priming stage of vacuole fusion (Fig. 3 G).

Docking, which leads to the stable association of membranes, can be subdivided into two stages: tethering, which requires the Rab GTPase Ypt7 and the multi-subunit homotypic fusion and protein sorting (HOPS vacuole)/class C-Vps complex (Price et al., 2000; Sato et al., 2000; Seals et al., 2000; Wurmser et al., 2000), is thought to facilitate the initial contacts between membranes. This is followed by trans-SNARE complex formation, which irreversibly connects membranes before lipid mixing (for review see Jahn et al., 2003). Docking can be assayed in vitro by adding FM4-64 to isolated vacuoles and observing vacuole clustering by microscopy (Mayer and Wickner, 1997). Even though wt vacuoles from galactose-grown cells are small (Fig. 3 H; Fig. S2 D), they form clusters in an ATP-dependent manner. GAL-*YCK3* vacuoles, in contrast, do not cluster, indicating that these vacuoles cannot dock (Fig. 3, H and I).

If vacuoles with extra Yck3 cannot dock, is better docking the reason why *yck3Δ* vacuoles fuse better? Inhibitors that block priming, HOPS function, SNARE complex formation, and downstream events had similar effects on wt and *yck3Δ* fusion (Fig. 4 A). Remarkably, though, two Ypt7 inhibitors,

when added as recombinant proteins to the fusion reaction, were unable to block fusion between *yck3Δ* vacuoles (Fig. 4 B). Neither the guanyl-nucleotide dissociation inhibitor Gdi1 (Haas et al., 1995), nor Gyp7-47, the normally highly potent active site of the Rab GTPase activating protein (GAP) Gyp7 (Eitzen et al., 2000), were able to block *yck3Δ* fusion, suggesting that the tethering stage is indeed altered in this mutant. Deletion of *yck3* did not appear to overcome the requirement for Ypt7/HOPS in tethering, because antibodies against Ypt7 and the HOPS subunit Vps41 (Fig. 4 A) both inhibited fusion, and both proteins are needed for *yck3Δ* vacuole biogenesis (Fig. S2 E). In confirmation of previous observations that Ypt7 (Haas et al., 1995; Mayer and Wickner, 1997) is required on both partner membranes, when Gdi1 or Gyp7-47 were added to fusion reactions between wt (susceptible) and *yck3Δ* (resistant) vacuoles, fusion was inhibited (Fig. 4 C). Thus, Yck3 affects the tethering stage of vacuole fusion.

#### Absence of *yck3* affects the in vivo distribution of the HOPS subunit Vps41

We analyzed the in vivo distribution of GFP-tagged proteins involved in tethering and later stages of vacuole fusion. GFP-Vps41 was strikingly enriched in punctate structures and vacuole interfaces in the *yck3Δ* strain, in contrast to wt cells (Fig. 5 A, arrows; Fig. S3, available at <http://www.jcb.org/cgi/content/full/jcb.200407141/DC1>). This suggests that, in *yck3Δ*, GFP-Vps41 is present in vacuole docking sites. GFP-Pho8 (a transmembrane protein not involved in fusion) is not enriched in these sites in either strain (Fig. 5 B), and other proteins—Ypt7 (Fig. 5 C), the Q-SNARE Vam3 (Fig. 5 D), and the late-acting fusion factor Vac8 (Fig. 5 E), each of which is known to be enriched at docking sites (Wada et al., 1997; Pan and Goldfarb, 1998; Wang et al., 2002)—are similarly distributed in both strains.

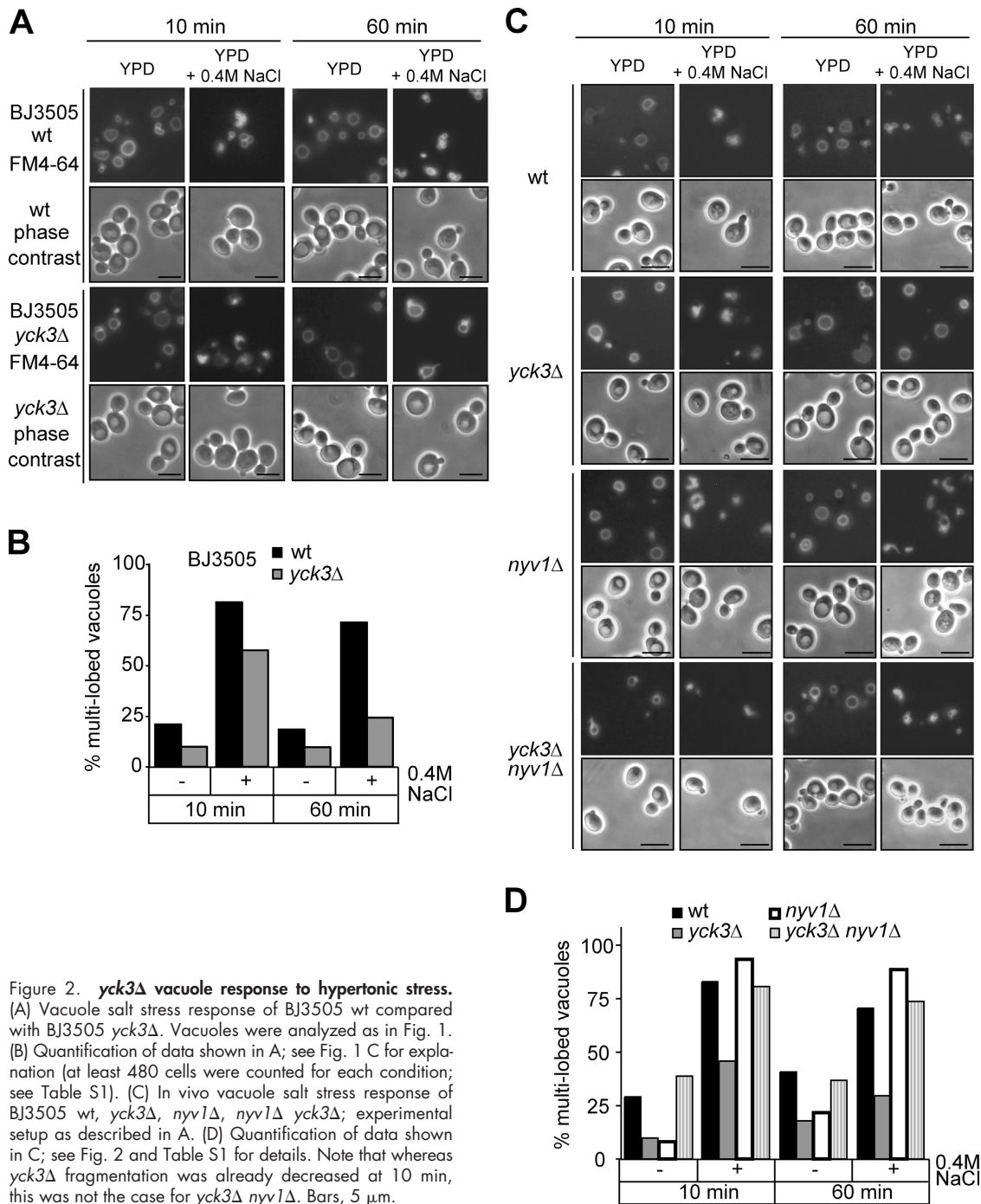


Figure 2. ***yck3Δ* vacuole response to hypertonic stress.** (A) Vacuole salt stress response of BJ3505 wt compared with BJ3505 *yck3Δ*. Vacuoles were analyzed as in Fig. 1. (B) Quantification of data shown in A; see Fig. 1 C for explanation (at least 480 cells were counted for each condition; see Table S1). (C) In vivo vacuole salt stress response of BJ3505 wt, *yck3Δ*, *nyv1Δ*, *nyv1Δ yck3Δ*; experimental setup as described in A. (D) Quantification of data shown in C; see Fig. 2 and Table S1 for details. Note that whereas *yck3Δ* fragmentation was already decreased at 10 min, this was not the case for *yck3Δ nyv1Δ*. Bars, 5  $\mu$ m.

### Yck3 is required for Vps41 phosphorylation

The above observations suggested to us a direct role for Yck3 in tethering complex modulation. Does Yck3 phosphorylate Vps41? Because we could not purify enough kinase or soluble Vps41 for in vitro phosphorylation studies, we took advantage of the fact that, when isolated vacuole fractions are incubated with ATP, Vps41 becomes retarded in its SDS-PAGE mobility (this study; Price et al., 2000). Is this due to Yck3 activity? We collected vacuole-containing fractions from wt and *yck3Δ* cells and found that the ATP-induced Vps41 up-shift is indeed dependent on Yck3 (Fig. 6 A). Of all class D or kinase deletion

mutants (Seeley et al., 2002) tested, including the other CKI isoforms (unpublished data), *yck3Δ* was the only strain completely abolished for the Vps41 up-shift, indicating a specific role for Yck3 in posttranslational modification of Vps41.

We purified modified Vps41 from vacuoles, and upon phosphatase treatment, it returned to its original gel mobility (Fig. 6 B), showing that the up-shift was due to phosphorylation. Interestingly, although Vps41 has 49 potential serine/threonine phosphorylation sites (NetPhos 2.0), its gel shift is completely dependent on Yck3 (Fig. 6). To demonstrate that Vps41 is an in vivo substrate for Yck3, we analyzed Vps41 phosphorylation in the GAL-*YCK3* strain. Indeed, in the presence of ex-

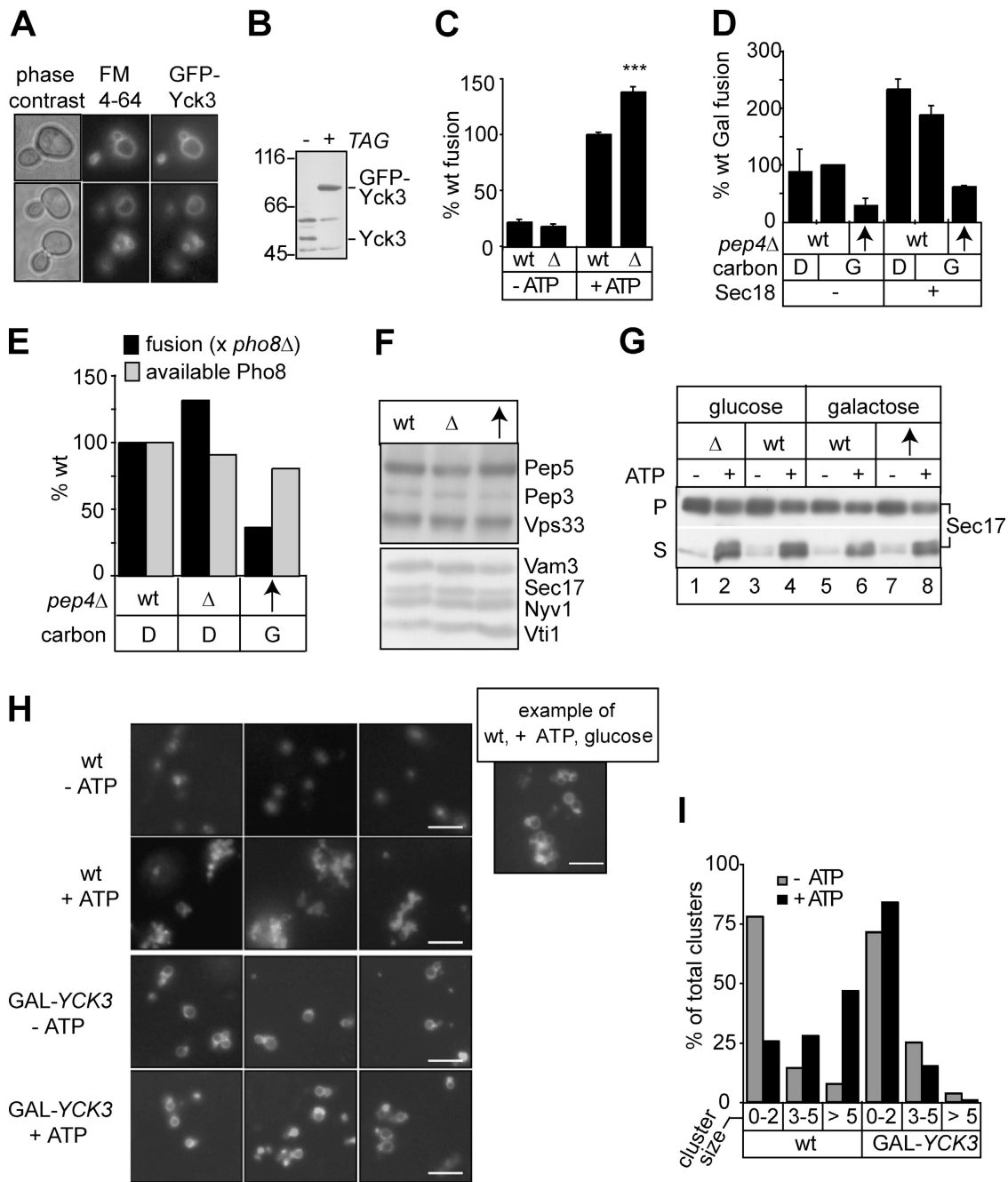


**Figure 3. Yck3 effect on in vitro vacuole fusion.** (A) Yck3 localization. BY4741 cells containing NH<sub>2</sub>-terminally GFP-tagged Yck3 were visualized by phase contrast, FM4-64 pulse-chase, and GFP fluorescence microscopy. (B) Comparison of untagged (–) and GFP-tagged (+) Yck3 protein in total extracts. (C) *yck3 $\Delta$*  vacuole fusion. The averaged results from BY4741 wt (*pep4 $\Delta$  x pho8 $\Delta$* ) and *yck3 $\Delta$*  (*yck3 $\Delta$  pep4 $\Delta$  x yck3 $\Delta$  pho8 $\Delta$* ) vacuole fusion assays were compared (wt + ATP = 100%: corresponds to an average of  $1.297 \pm \text{SD } 0.595$  ALP units). Error bars are standard errors from at least 30 independent experiments; according to *t* test, –ATP experiments,  $P = 0.1754$ ; +ATP,  $***P < 0.0001$ ;  $\Delta$ , *yck3 $\Delta$* . (D) Yck3 over-production effect on vacuole fusion. Vacuoles from the indicated *pep4 $\Delta$*  strains (wt or YCK3 overexpressed under the GAL promoter [arrows]) were isolated from cultures grown with glucose (D) or galactose (G) as carbon source, and fused with *pho8 $\Delta$*  vacuoles (from YPD-grown cultures –*pho8 $\Delta$*  vacuoles from all galactose-grown cultures were fusion incompetent; Fig. S2), in the absence (–) or presence (+) of recombinant Sec18 (400 ng/ml). Fusion is set to 100% for *pep4 $\Delta$*  wt, from cells grown in galactose (error bars are SD from six independent experiments). (E) Comparison of vacuole fusion (as in D) and available ALP reporter (as measured by Pho8 enzymatic activity; see Materials and methods) among wt, *yck3 $\Delta$*  ( $\Delta$ ), and GAL-YCK3 (arrow) vacuoles from the BY4741 *pep4 $\Delta$*  background; BY4741 *pho8 $\Delta$*  was the fusion partner. (F) Protein comparison among the *pep4 $\Delta$*  vacuoles used in E. Wt, *yck3 $\Delta$*  ( $\Delta$ ), and GAL-YCK3 (arrow) vacuoles were analyzed by Western blot. (G) Priming of *yck3 $\Delta$* , wt, and GAL-YCK3 vacuoles. Fusion reactions containing BY4741 *pep4 $\Delta$*  vacuoles (4  $\mu\text{g}$ ) from the indicated strains/carbon sources (abbreviated as in D and E) were incubated for 15 min in the absence (–) or presence (+) of ATP and recombinant Sec18 (400 ng/ml). Vacuoles were reisolated, and Sec17 release was assayed by SDS-PAGE and Western blot (Mayer et al., 1996). P, reaction pellet (vacuoles); S, reaction supernatant. (H) Docking of GAL-YCK3 vacuoles. Isolated *pep4 $\Delta$*  wt and *pep4 $\Delta$*  GAL-YCK3 vacuoles from cells grown in galactose were incubated in the following reactions: 5  $\mu\text{g}$  vacuoles, 40 mM KCl, 1 mM MgCl<sub>2</sub>, 5 mg/ml cytosol, 30  $\mu\text{M}$  FM4-64, in PS buffer, in the absence or presence of reduced ATP regenerating system (0.3 mM ATP instead of the usual 0.5 mM; modified from Mayer and Wickner, 1997). After 30 min at 27°C, 2  $\mu\text{l}$  of the reaction was mixed with 0.4% agarose, mounted on ice-cold glass slides, and analyzed by fluorescence microscopy. Bars, 10  $\mu\text{m}$ . The inset shows an example of wt vacuoles (after 30 min fusion +ATP) from the experiment in Fig. S2 A, to give an impression of wt docking when cells are grown in glucose. (I) Quantification of experiment in H: a cluster refers to a single group of vacuoles in the field; cluster size refers to the number of vacuoles in that group. At least 130 clusters were counted for each condition.

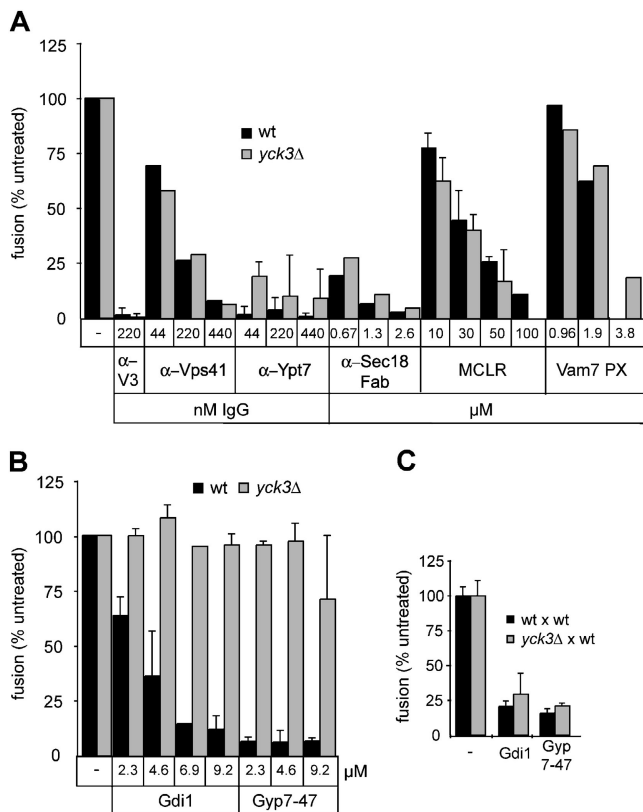


Figure 4. **Effect of *yck3* deletion on vacuole fusion.** (A) Susceptibility of wt and *yck3Δ* fusion to stage-specific inhibitors. Standard fusion reactions, as described in Fig. 3 C, contained the indicated inhibitors; fusion was compared with control reactions of the respective vacuoles without inhibitor (set to 100%). α-V3, anti-Vam3; MCLR, microcystin LR (a late-stage inhibitor of vacuole fusion). SD,  $n = 2-5$ . (B) Effect of Ypt7 inhibitors on *yck3Δ* vacuole fusion. Fusion reactions (as in A) contained Gdi1 or the GAP fragment, Gyp7-47 (SD,  $n = 3-7$ ). (C) Requirement for Ypt7 on both fusion partners. Wt or *yck3Δ* vacuoles (each *pep4Δ*) were fused against wt *pho8Δ* vacuoles, in the presence of 9.2 μM Gdi1 or 4.6 μM Gyp7-47; fusion was compared with control reactions without inhibitor (SD,  $n = 2$ ).

cess Yck3 (Fig. 6 C, bottom), Vps41 was constitutively phosphorylated (Fig. 6 C, top, and D). Further substantiating a direct connection between Yck3 and Vps41, we found that they are associated on isolated vacuoles (Fig. 6 E). We also observed that Vps41 on *yck3Δ* vacuoles is a competent Yck3 substrate: when Yck3<sup>+</sup> vacuoles containing tagged Vps41 were incubated together with *yck3Δ* vacuoles containing untagged Vps41, untagged Vps41 became phosphorylated in trans (Fig. 6 F).

### Yck3 influences HOPS's association with membranes

Gdi1 and Gyp7-47 are unable to inhibit *yck3Δ* vacuole fusion (Fig. 4 B). Previous analysis of vacuole tethering has shown that, after priming, the HOPS complex becomes associated with Ypt7 (Price et al., 2000). Thus, when vacuoles are incubated with ATP, Gdi1 and Gyp7-47 can extract the HOPS subunits Vps41 and Vam6, presumably because they lose their receptor on the membrane. This extraction requires two ATP-dependent steps: priming, and a second, unknown step (Price et al., 2000). In addition, a recent study found that an excess of the Q-SNARE Vam7 can overcome the ATP-requirement

(priming) for vacuole fusion. This ATP-independent fusion reaction is resistant to inhibition by Gdi1 (Thorngren et al., 2004). We hypothesized that this step might be Yck3 phosphorylation of Vps41. To test this, we incubated isolated vacuoles with ATP and either Gdi1 or Gyp7-47 and analyzed Vps41 binding. As shown in Fig. 7 (A and B), in the presence of ATP, Vps41 becomes partly released from wt vacuoles (in a reaction enhanced by Gyp7-47/Gdi1), but not from *yck3Δ* vacuoles. The release of another HOPS subunit, the Ypt7 guanine nucleotide exchange factor (GEF) Vam6 (Wurmser et al., 2000), is also dependent on Yck3 (Fig. 7 C). This is not, however, the case for Gdi1-dependent extraction of Ypt7: it is as efficiently extracted from *yck3Δ* vacuoles as from wt membranes (Fig. 7 B). Given that *yck3Δ* vacuole fusion is not inhibited by Gdi1 or Gyp7-47, and the HOPS subunits Vps41 and Vam6 are more stably associated with these vacuoles, we suggest that HOPS-associated Ypt7 on *yck3Δ* vacuoles is more active than on wt vacuoles.

### Vps41 undergoes Yck3-dependent phosphorylation in vivo during hypertonic stress

Based on the above observations, we hypothesized that Yck3 might phosphorylate Vps41 in order to block tethering during hypertonic stress. As shown in Fig. 8 (A and B), 30–40% of total cellular Vps41 became phosphorylated upon moving cells from YPD to 0.9 M NaCl, whereas Vps41 in *yck3Δ* cells was not phosphorylated; *yck3Δ* vacuoles do become large again in vivo even in 1 M NaCl (Fig. S4, available at <http://www.jcb.org/cgi/content/full/jcb.200407141/DC1>). Interestingly, when wt cells were relieved of salt stress, phosphorylation was immediately reversed (Fig. 8 B). It is plausible that rapid dephosphorylation of Vps41 permits the reestablishment of docking sites and resumption of membrane fusion. In support of this, GFP-Vps41 is dramatically enriched at interfaces between fragmented *yck3Δ* vacuoles when cells are hypertonically shocked (Fig. 8 C).

### yck3 deletion interferes with vacuole inheritance

What do these results imply for vacuole behavior in unstressed, normally growing cells? We observed that salt-induced vacuole fragmentation resembles the formation of vacuole inheritance structures (Fig. 2; Fig. S1). Moreover, several vacuole mutants that cannot fragment during hypertonic stress also fail to form segregation structures and are thus defective in vacuole inheritance (this study; Raymond et al., 1990; Y.X. Wang et al., 1996; Gomes de Mesquita et al., 1996; Bonangelino et al., 1997; Weisman, 2003). Therefore, we asked whether Yck3-mediated vacuole fusion inhibition is also needed for the maintenance of segregation structures, and found that *yck3Δ* cells had a pronounced inheritance defect: ~50% of *yck3Δ* cells, compared with ~80% of wt cells, had labeled vacuoles in their buds after a long chase period (Table III; Fig. 9). Furthermore, the *yck3Δ* vacuoles that were inherited were often reduced in size compared with wt, and tubulo-vesicular segregation structures were not observed; Fig. 9, arrows in wt). Strikingly, many *yck3Δ* cells lost their dye label over time, which is consistent with a

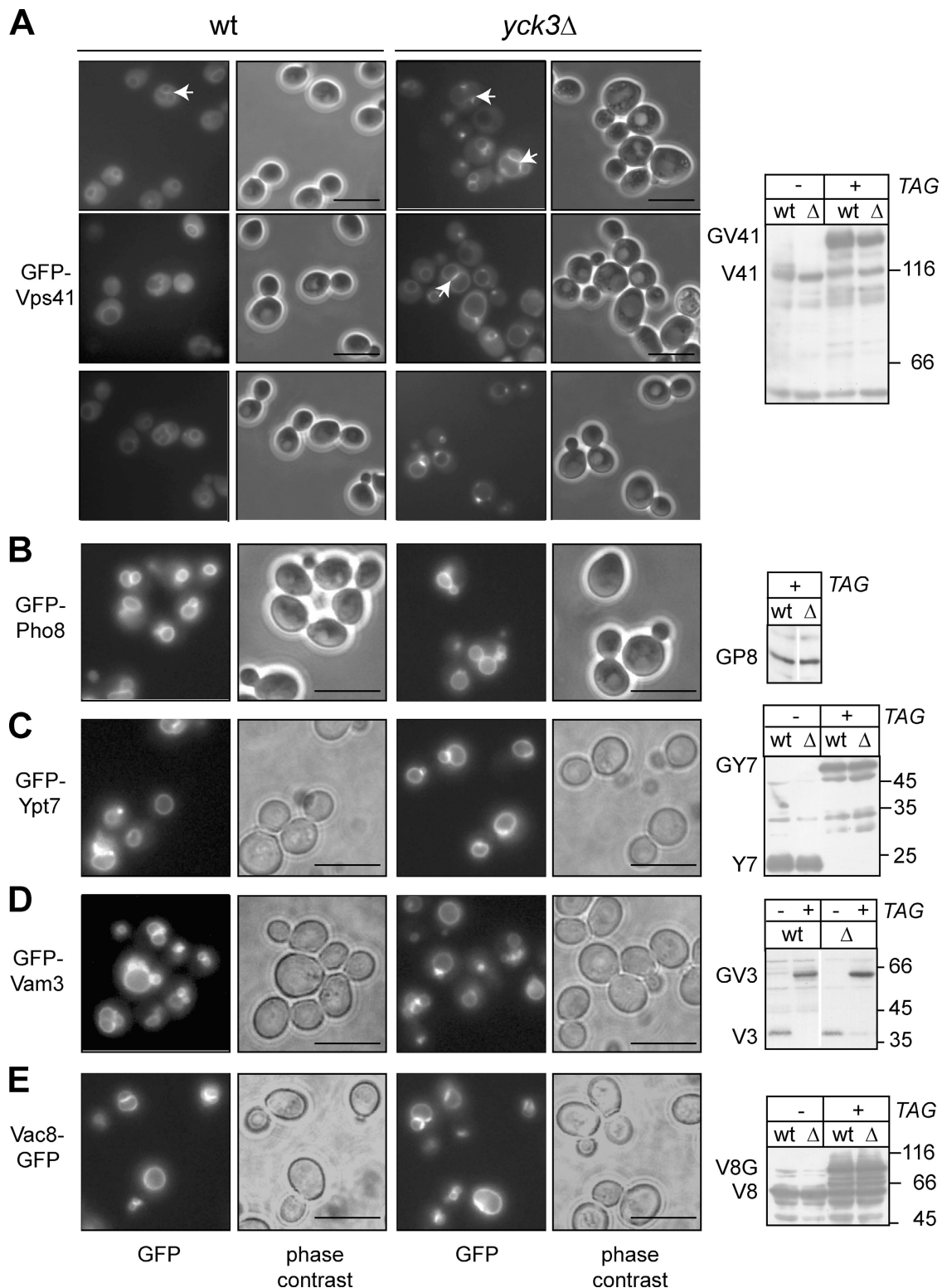
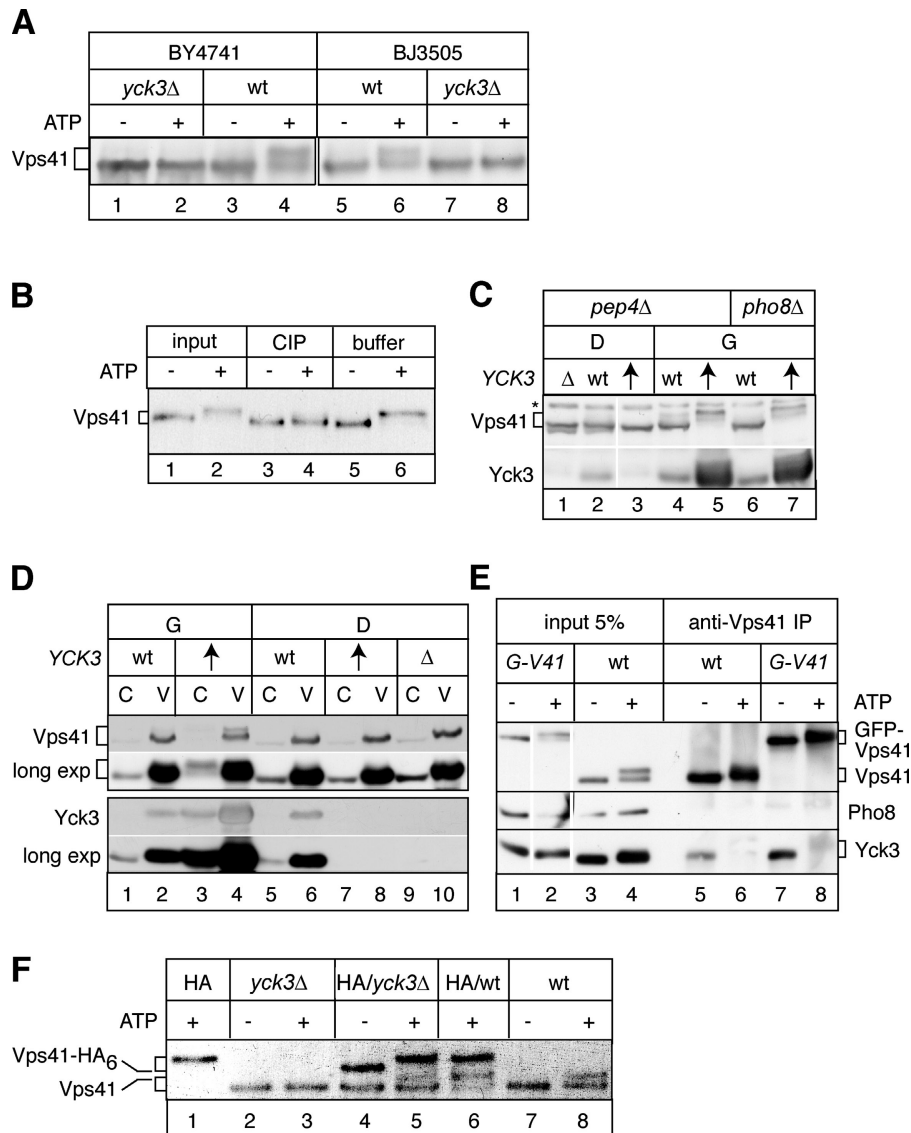


Figure 5. **Effect of *yck3* deletion on localization of GFP-tagged vacuolar proteins.** (A) GFP-Vps41 localization in vivo. NH<sub>2</sub>-terminally GFP-tagged Vps41 was introduced into BY4741 *pho8Δ* (wt) and BY4741 *yck3Δ*, and cells were visualized by fluorescence microscopy. Arrows indicate examples of vacuole interfaces (see also Fig. S3). Western blot analysis of proteins from total extracts is shown, Δ = *yck3Δ*; numbers indicate molecular weight. (B–E) Localization of other vacuolar proteins. NH<sub>2</sub>-terminally GFP-tagged proteins in BY4741 wt and *yck3Δ* (B–D), and COOH-terminally GFP-tagged Vac8 in BY *pho8Δ* (wt) and *yck3Δ* (E); for each, localization and expression (with and without GFP tags) are shown, as described in A. Bars, 5 μm.

defect in vacuole inheritance (Fig. 9; Table III, compare 45-min and 4–5-h chase). These defects in *yck3Δ* vacuole inheritance are less severe than in mutants deleted for inheritance machin-

ery (*vac8Δ*, *vac17Δ*; Wang et al., 1998; Tang et al., 2003), and, indeed, inheritance in the *yck3Δ vac8Δ* mutant was nearly abolished (Table III, not depicted). These data exclude Yck3 as vac-



**Figure 6. Yck3 dependence of Vps41 phosphorylation.** (A) Vps41 mobility shift in vitro. P13 membrane fractions from the indicated strains were incubated in 150  $\mu$ l reactions with or without ATP under standard fusion conditions for 30 min. Membranes were reisolated and Vps41 was analyzed by Western blotting. (B) Vps41 phosphorylation. BJ3505 wt vacuoles were incubated in fusion reactions with or without ATP. Vacuoles were reisolated, and Vps41 was purified by denaturing immunoprecipitation. Eluted protein was then left untreated (input), treated with calf intestinal ALP (CIP), or with CIP buffer only. Vps41 was analyzed by SDS-PAGE and Western blotting. (C) In vivo phosphorylation of Vps41. BY4741 cells (*yck3Δ* [ $\Delta$ ], YCK3 wt [wt], or GAL-YCK3 [arrows]) carrying fusion reporter gene deletions (*pep4* or *pho8*) were grown to log phase in glucose (D) or galactose (G), and lysed as described in Materials and methods. Proteins were analyzed by Western blot. The asterisk indicates a cross-reacting band. Lanes 1 and 2 are from the same gel as lanes 3–7. (D) Yck3 enrichment on vacuoles and Vps41 phosphorylation. Vacuoles (V) from the indicated strains/growth conditions (abbreviated as in C) were prepared as in Materials and methods, except that aliquots of total lysate (C = cells) were removed before gradient centrifugation. Cells/vacuoles were diluted in PS buffer with protease inhibitors, subjected to TCA precipitation (13% vol/vol) and 100% acetone wash, and 60  $\mu$ g cells/30  $\mu$ g vacuoles were loaded on SDS-PAGE and analyzed by Western with anti-Vps41 (top; a long exposure is also shown) followed by anti-Yck3. (E) Vps41/Yck3 complex formation. Vacuoles (80  $\mu$ g) from BJ3505 with (G-V41) or without (wt) GFP-tagged Vps41 were incubated in 400  $\mu$ l fusion reactions containing protease inhibitors (Complete Mini, EDTA-free) with or without ATP for 30 min. Reactions were then processed for coimmunoprecipitation with protein A Sepharose (Amersham Biosciences)-coupled Vps41 antibodies as described in Veit et al. (2001). Eluted proteins and the 5% loading control were then analyzed by SDS-PAGE and Western blot with anti-Yck3, Vps41, and Pho8 antibodies. Lane 2 is from a different gel from the same experiment. (F) Cross-phosphorylation of Vps41. Vacuoles from BJ3505 Vps41-HA<sub>6</sub> (HA), BY4741 *pep4Δyck3Δ*, or BY *pep4Δ* (wt) (12  $\mu$ g each) were incubated alone (lanes 1–3, 7, and 8) or together (lanes 4–6) in fusion reactions with or without ATP. After 1 h, vacuoles were diluted in PS with 150 mM KCl (PSK), reisolated, and proteins were analyzed as in A.

teins and the 5% loading control were then analyzed by SDS-PAGE and Western blot with anti-Yck3, Vps41, and Pho8 antibodies. Lane 2 is from a different gel from the same experiment. (F) Cross-phosphorylation of Vps41. Vacuoles from BJ3505 Vps41-HA<sub>6</sub> (HA), BY4741 *pep4Δyck3Δ*, or BY *pep4Δ* (wt) (12  $\mu$ g each) were incubated alone (lanes 1–3, 7, and 8) or together (lanes 4–6) in fusion reactions with or without ATP. After 1 h, vacuoles were diluted in PS with 150 mM KCl (PSK), reisolated, and proteins were analyzed as in A.

uole inheritance machinery per se, but strongly indicate that it is needed to ensure the fidelity of this trafficking event.

## Discussion

### Identification of the tethering regulator Yck3 in a screen for vacuole morphology control

In this study, we analyzed yeast vacuole fragmentation during hypertonic stress in order to identify genes that regulate organelle morphology (Fig. 1; Table II). We confirmed the requirement for PtdIns(3,5)P<sub>2</sub> synthesis in the initial vacuole volume decrease, and found *VPS3*, a gene required for vacuole biogenesis and inheritance (Raymond et al., 1990), to also be involved in this process. Furthermore, we showed that budding yeast vacuole fragmentation in response to hypertonic stress is,

in contrast to the fission yeast *Schizosaccharomyces pombe* (Bone et al., 1998), independent of the Hog1 MAPK pathway. Because vacuoles in these two organisms differ dramatically in morphology (fission yeast vacuoles are typically small and numerous), it is likely that they use different mechanisms for membrane remodeling.

As a result of this screen, we identified a previously uncharacterized vacuolar kinase, the CKI isoform Yck3. Deletion of *yck3* had an interesting effect on vacuole morphology during salt stress: while vacuoles were able to undergo the initial decrease in volume, they became large again in a SNARE-dependent manner (Fig. 1 C; Fig. 2; Fig. 8 C), leading us to hypothesize that Yck3 prevents vacuoles from refusing during hypertonic stress. It makes sense that such a mechanism would be required. When cells are exposed to an increase in environmental salt, they need to maintain the osmotic balance of the

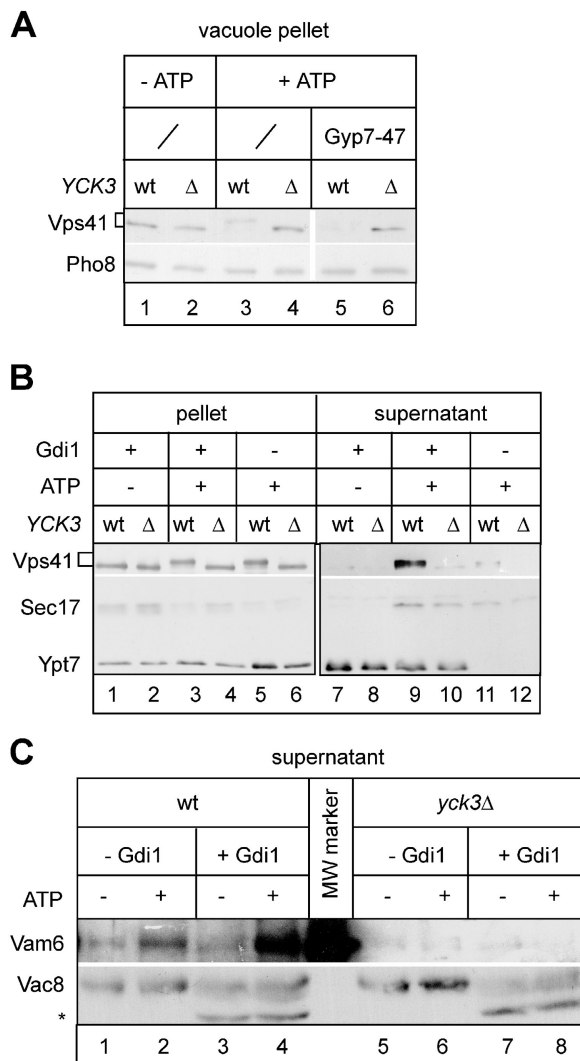


Figure 7. **HOPS association with *yck3* $\Delta$  vacuoles.** (A) Release of Vps41 from membranes. BY4741 *pep4* $\Delta$  vacuoles (wt or *yck3* $\Delta$ ) were incubated in 75- $\mu$ l fusion reactions (15- $\mu$ g vacuoles) containing protease inhibitors,  $\pm$ ATP,  $\pm$ 4.6  $\mu$ M Gyp7-47 for 45 min. Reactions were then diluted in PSK buffer, and vacuoles were reisolated by centrifugation and analyzed by Western blot with the indicated antibodies. Lanes 1–4 and 5–6 are all from the same gel. (B) Recovery of Vps41 in the supernatant. Isolated vacuoles from BY4741 *pep4* $\Delta$  (wt) and BY4741 *pep4* $\Delta$  *yck3* $\Delta$  ( $\Delta$ ) were incubated in 60  $\mu$ l standard fusion reactions containing, when indicated, ATP and/or recombinant Gdi1 (9.2  $\mu$ M) for 30 min. Vacuoles were reisolated, and pellets (1/2) and TCA-precipitated supernatants (all) were analyzed as in A. (C) Reactions as in B. Supernatants were precipitated, and analyzed by Western blotting using the antibodies indicated. Asterisk indicates a cross-reacting band from Gdi1. The 116-kD band of the molecular mass marker also produces a cross-reacting signal.

cytosol. Therefore, the large vacuole quickly releases water by membrane fission through a process that involves transient phospholipid remodeling (Dove et al., 1997; Bonangelino et al., 2002b). Because a subsequent increase in vacuole volume would disturb the cytosolic homeostasis just achieved, a second response might be that vacuole fusion is also actively prevented. This could keep the cells alive until either the environment returns to normal or the cytosolic glycerol content increases via activation of the Hog1 pathway (Mager and Siderius, 2002; Weisman, 2003).

To confirm the role of Yck3 as a potential negative regulator of vacuole fusion, we showed that in vitro vacuole fusion is increased when Yck3 is absent, and blocked at the docking stage when overproduced (Fig. 3). This, together with our striking observation that vacuole fusion becomes resistant to Rab GTPase inhibitors when *yck3* is deleted (Fig. 4 B), suggests that Yck3 is a regulator of vacuole tethering. In support of this possibility, we found that Yck3 is specifically needed for the phosphorylation of the HOPS tethering subunit Vps41 (Fig. 6). When Vps41 cannot be phosphorylated, its membrane association is altered: it accumulates at vacuole docking sites in vivo (Fig. 5 A; Fig. 8 C) and, along with the HOPS complex subunit/Rab-GEF Vam6, cannot be released from membranes in vitro (Fig. 7). We propose that, through Vps41 phosphorylation, Yck3 controls the activation state of the Rab Ypt7: Vps41 phosphorylation decreases the Rab/HOPS interaction on vacuoles, leading to reduced HOPS-associated GEF activity and increased access of the Rab-GAP and Gdi1. Thus, under conditions when Yck3 is more active, more Vps41 becomes phosphorylated, and causing tethering complex inactivation and fusion inhibition; by this, fragmented vacuoles stay fragmented. If Yck3's activity is reduced, Vps41 and Vam6 are more stably associated with Ypt7, tethering is efficient, and fusion proceeds.

In support of our model, we found that Vps41 phosphorylation and vacuole fragmentation during hypertonic stress are indeed correlated in vivo (Fig. 8). Despite the strength of this correlation and its attractiveness as a model, we acknowledge that Yck3 may regulate tethering through multiple substrates, as this stage of vacuole fusion involves many factors in several, inter-connected complexes (Müller et al., 2002; Wickner, 2002; Wang et al., 2003). We have not yet been able to determine the exact relationship between Vps41 and Yck3 in regulating vacuole fusion and architecture, because Vps41 is essential for several stages of vacuole biogenesis (see below), including transport of Yck3 itself (unpublished data).

#### Tethering complexes as control centers for regulation of membrane dynamics

It is fitting that the HOPS tethering complex would be an important locus for integration of environmental/developmental signals with vacuole fusion regulation. Vesicle tethering complexes, as effectors of small GTPases of the Rab/Ypt family, have been hypothesized to regulate the specificity and timing of membrane fusion (for reviews see Zerial and McBride, 2001; Whyte and Munro, 2002), although we still lack a satisfying picture of how tethering is accomplished, let alone regulated. Further adding to their potential (and complexity), putative tethering complexes seem to have diverse roles in membrane trafficking. Each of the six subunits of the HOPS complex, for example, is required for several pathways of vacuole biogenesis, and deletion of individual genes causes cells to become temperature sensitive for growth and defective in other membrane transport events (Wada et al., 1992; Rieder and Emr, 1997; Srivastava et al., 2000; Wurmser et al., 2000; Peterson and Emr, 2001). Vps41 is especially optimal as a control center module, as it seems to be involved in fusion and

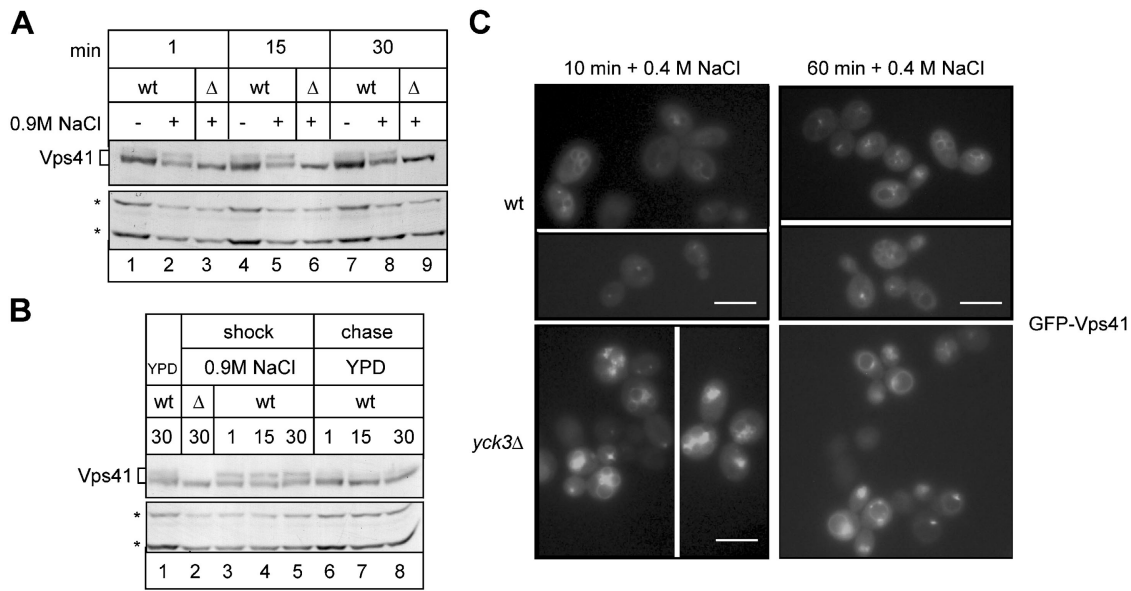


Figure 8. **Hypertonic stress effect on Vps41 in vivo.** (A) Vps41 phosphorylation upon salt stress. BJ3505 cells (wt and *yck3Δ*) from logarithmically growing YPD cultures were collected and transferred to YPD with or without 0.9 M NaCl, and grown for the indicated times. At each time point, 0.25 OD<sub>600</sub> U from the culture was collected, immediately lysed as described in Materials and methods, and analyzed by Western blotting. Asterisks on the bottom panel indicate cross-reacting bands. (B) Vps41 dephosphorylation upon removal of salt stress. Cells were salt stressed as in A. After 30 min, cells were collected, washed twice in YPD, resuspended in YPD to the density before washing, and incubated for the indicated times. Lysis and analysis was as in A. (C) GFP-Vps41 localization during osmotic stress. BY4741 strains (wt or *yck3Δ*) carrying *GFP-VPS41* on a centromeric vector were incubated in SD-Leu + 0.4 M NaCl for the indicated times and then analyzed by fluorescence microscopy. Bars, 5  $\mu$ m.

fission. As part of the HOPS complex, it regulates vacuole fusion (Price et al., 2000; Wurmser et al., 2000). Through its interaction with the AP-3 complex, Vps41 is needed to form Golgi-derived vesicles that follow the alkaline phosphatase (ALP) pathway to the vacuole (Piper et al., 1997; Rehling et al., 1999; Darsow et al., 2001). This pathway transports ALP (the *PHO8* gene product) and a subset of vacuolar SNAREs

(for review see Mullins and Bonifacino, 2001), although the functional significance of this seemingly minor, nonendosomal route to the vacuole is still not clear. Might this pathway also be important for vacuole budding/fragmentation? Perhaps Yck3 flicks a fusion-to-fission switch. Phosphorylated Vps41 might change its contacts on the vacuole membrane, causing it to participate in budding while distracting it from its fusion

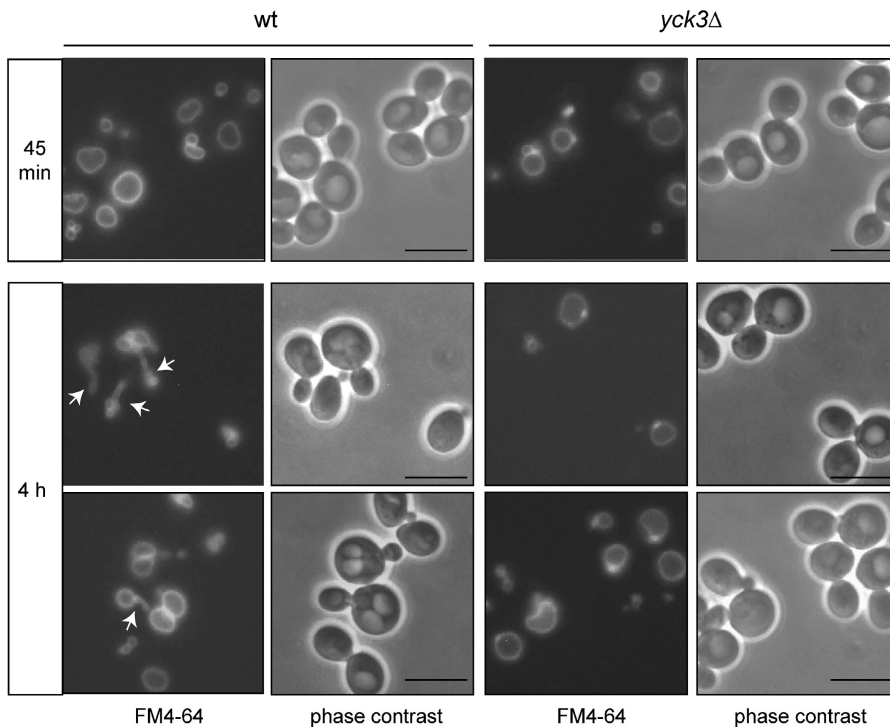


Figure 9. **Effect of *yck3* deletion on vacuole inheritance.** Vacuole inheritance in BJ3505 wt and *yck3Δ* was analyzed by pulse chase with FM4-64 (chase durations are indicated) and fluorescence microscopy as described in Materials and methods. See Table III for quantification. Arrows indicate inheritance structures. Bars, 5  $\mu$ m.

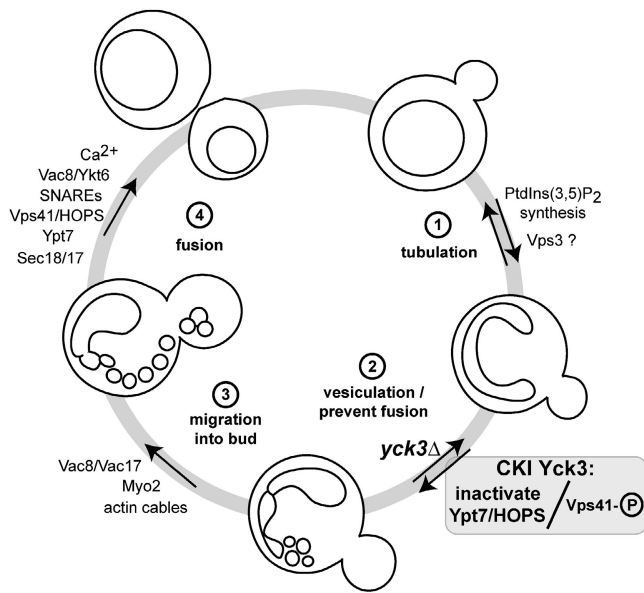


Figure 10. **Model of changes in vacuole architecture during inheritance.** The cycle depicts the stages of vacuole fragmentation and fusion during the cell cycle. Reactions and components implicated at each step are listed. For details see text.

role. In this context, it is noteworthy that all four budding yeast CKI isoforms can regulate small GTPases involved in vesicle formation. In one report, Yck1/2/3 overexpression compensated for an ARF-GAP deletion (X. Wang et al., 1996); in another study, inactivation of Hrr25 rescued a SAR-GEF defect in ER-Golgi transport (Murakami et al., 1999). Based on all this, we propose that organelle-specific CKI isoforms promote remodeling of the tethering/coat complexes in which these GTPases are embedded. CKI isoforms might therefore play a critical role in fine-tuning small GTPase function, perhaps even coordinating fusion/fission regulation.

### A common mechanism for changes in organelle architecture

Yck3 is needed to maintain vacuole fragmentation in response to high environmental salt and is also required for efficient vacuole inheritance (Fig. 9), suggesting that it plays a similar role in both pathways.

We propose a general model for regulated changes in vacuole morphology, using the framework of cell cycle-controlled vacuole inheritance (Fig. 10): early in G1, vacuoles extend tubules via lipid remodeling (step 1). This depends on (a) generation of PtdIns(3,5)P<sub>2</sub> from PI(3)P and (b) Vps3. Because PtdIns(3,5)P<sub>2</sub> levels can fluctuate (Dove et al., 1997), this step is reversible. As tubules extend, they pinch off vesicles, which must be prevented from fusing back (step 2). Phosphorylation by Yck3 of Vps41 (and possibly other proteins) is required at this stage, in order to block HOPS-mediated tethering and prevent homotypic vacuole fusion (as well as transport vesicle-to-vacuole fusion). We speculate that Yck3 phosphorylation of Vps41 also transforms it into a budding factor. In the absence of *yck3*, this stage is reversible: vesicles might pinch off, but they fuse back, and inheritance becomes a challenge. In the presence of active Yck3, however, these vesicles accumulate, and attach to actin filaments through the interaction of Vac8, Vac17, and the type V myosin, Myo2 (step 3; Tang et al., 2003). Thus anchored to the cytoskeleton, vacuole fragments migrate vectorially into the bud, where they fuse, reassembling the large vacuole (step 4).

The above model of vacuole inheritance has clear parallels to mitotic Golgi division in mammalian cells (for reviews see Shorter and Warren, 2002; Colanzi et al., 2003): before mitosis, the normally stacked cisternae detach and form tubules, which then fragment into vesicles. These vesicles are prevented from refusing by the same mechanism that unstacks the cisternae: phosphorylation of matrix proteins, including the vesicle tethering factor GM130, by cell cycle-controlled kinases (Lowe et al., 1998). The Golgi fragments are then distributed

Table III. **Effect of *yck3* deletion on vacuole inheritance**

Chase duration	Strain	Budded <sup>a</sup>						Unbudded						% Budded	Total n <sup>c</sup>
		%	n <sup>b</sup>	%	n	%	n	%	n	%	n				
30–45 min	wt (BJ)	82	183	16	35	1.8	4	99	317	1.6	5	41	544		
	<i>yck3Δ</i> (BJ)	54	143	44	118	1.9	5	95	264	5.4	15	49	545		
4–5 h	wt (BJ)	87	203	11	25	2.2	5	97	100	2.9	3	69	336		
	<i>yck3Δ</i> (BJ)	45	64	40	57	15	22	56	43	44	34	65	220		
	wt (BY)	89	284	10	32	0.94	3	94	188	6.5	13	61	520		
	<i>yck3Δ</i> (BY)	49	73	28	41	24	35	54	39	46	33	67	221		
	<i>pho8Δ</i> (BY)	72	184	17	43	11	29	85	71	15	13	75	340		
	<i>pho8Δ yck3Δ</i> (BY)	53	76	26	38	21	30	53	17	47	15	82	176		
	<i>vac8Δ</i> (BY)	0	0	50	18	50	18	0	0	100	11	77	47		
	<i>vac8Δ yck3Δ</i> (BY)	10	3	43	13	47	14	29	4	71	10	68	44		

<sup>a</sup>Budded and unbudded cells were quantified separately.

<sup>b</sup>Number of cells having the indicated phenotype.

<sup>c</sup>Budded cells compared with unbudded cells, from a “total n” number of cells counted from that condition and strain. Data are from the following numbers of experiments: 30–45-min chase, BJ wt/*yck3Δ* (4); 4–5-h chase, BY wt/*yck3Δ* (2), and others (1).

between nascent daughter cells, and, late in mitosis, fusion is resumed and a stacked Golgi is reestablished. Thus, fragmentation of both Golgi and yeast vacuoles is accompanied by tethering complex phosphorylation and inactivation, and the consequent inhibition of membrane fusion. By this, vesicles accumulate, which can be distributed between nascent cells.

In conclusion, we found that the CKI Yck3 acts on the HOPS tethering complex to negatively regulate vacuole fusion. In doing so, it exerts influence over vacuole assembly and disassembly, and thus controls vacuole architecture. Our findings, together with our current knowledge of Golgi inheritance, lead us to propose that tethering complex phosphorylation is a general mechanism for reversible fusion inhibition during organelle remodeling.

## Materials and methods

See figure legends for methods not described here. For yeast strains (listed in Table I) and plasmid construction see Online supplemental materials.

### Microscopy

FM4-64 (Molecular Probes) pulse-chase analysis of whole cells was as previously described. Vacuole inheritance experiments were according to Catlett and Weisman (1998), and other labeling experiments were done as in Vida and Emr (1995). Vacuoles were visualized by phase contrast and fluorescence microscopy as described below, using the filter set 23.

For GFP microscopy, cells were grown to mid-log phase in filter-sterilized SD medium supplemented with all amino acids (except Vac8-GFP [Fig. 5 E] and GFP-Vps41 in Fig. 8 C, in which SD-Leu was used). Cells were washed and resuspended fresh medium, an aliquot was placed onto a glass slide, covered with a coverslip, and immediately analyzed at RT. Images were acquired with a Zeiss Axiovert 35 microscope equipped with AxioCam, with filter set 10 or phase contrast, with a 100 $\times$  objective. Color images were acquired with Zeiss AxioVision 3.1 software, and processed using Adobe Photoshop 7.0. Figures show representative fields from multiple experiments.

### Biochemical reagents

All biochemical reagents were purchased from Sigma-Aldrich or Roth, unless indicated. All reagents added to vacuoles were prepared in, or dialyzed into, 10 mM Pipes-KOH, pH 6.8, 200 mM sorbitol (PS) buffer.

### Antibodies

All antibodies used in this study were rabbit polyclonal as described previously (Veit et al., 2001). Antibodies against His<sub>6</sub>-tagged Vps41, Vam6 (Price et al., 2000), and Pho8 were provided by W. Wickner (Dartmouth Medical School, Hanover, NH). IgGs, Fab fragments, and affinity purified antibodies were prepared as described previously (Price et al., 2000); anti-Yck3 was raised in rabbits against the kinase domain of Yck3 (aa 1–333), fused to a GST tag and purified from *E. coli* (using the pGEX4T3-Yck3NTD vector), and affinity purified with an Affi-Gel 10 (Bio-Rad Laboratories) column containing GST-Yck3(1–333).

### Total protein extraction from yeast

To analyze protein content of yeast cells, cells were lysed in 0.25N NaOH, 140 mM  $\beta$ -ME, 3mM PMSF, followed by 50% TCA precipitation, and acetone wash; equal amounts (0.25–0.5 OD<sub>600</sub> equivalents of cells) were analyzed by Western blot. For extractions in which Vps41 phosphorylation was analyzed, 0.25 OD<sub>600</sub> U of cells in mid-log phase were lysed as above, but with the addition of Complete Mini protease inhibitor cocktail (PIC; Roche; 1 tablet/12 ml of buffer), and phosphatase inhibitors (50 mM NaF, 0.1 mM sodium orthovanadate, 5 mM  $\beta$ -glycerophosphate).

### Membrane fractionation

Cultures (20 ml) were grown to OD<sub>600</sub> = 0.8–1.0 in YPD. Until lysis, cells were treated as for the vacuole purification, adjusted relative to the smaller culture size. Spheroplasts were resuspended in 1 ml of lysis buffer (200 mM sorbitol, 50 mM KOAc, 2 mM EDTA, 20 mM Hepes-KOH pH 6.8, 1 $\times$  PIC [Haas, 1995], 1 mM PMSF, 1 mM DTT), and cells were os-

motically lysed in DEAE-dextran/HCl. The total extract was centrifuged at 400 g, 5 min, 4°C, and the supernatant (S4) was then centrifuged for 15 min at 13,000 g. The “P13” pellets were collected and diluted to 0.3–0.4 mg/ml in PS buffer containing 0.1 $\times$  PIC.

### In vitro vacuole fusion

Vacuoles (purified according to Haas et al., 1995) or P13 fractions were incubated at 26°C in PS buffer supplemented with salts (Mayer et al., 1996; 0.5 mM MgCl<sub>2</sub>, 0.5 mM MnCl<sub>2</sub>, 125 mM KCl), CoA (10  $\mu$ M), with or without an ATP-regenerating system (0.5 mM ATP, 40 mM creatine phosphate, 0.1 mg/ml creatine kinase). Where indicated, reactions also contained recombinant Gdi1, His<sub>6</sub>-Sec18, GST-Vam7 PX domain (aa 1–122; Boedinghaus et al., 2002), or Gyp7-47-His<sub>6</sub> [Eitzen et al., 2000].

Vacuole fusion using BY4741 *pep4 $\Delta$*  and *pho8 $\Delta$*  vacuoles was measured by a biochemical complementation assay as described previously (Haas, 1995). Fusion was determined by measuring the absorbance of at least duplicate samples at 400 nm. Except where indicated, the results are expressed by subtracting the signal from an incubation lacking ATP. 1 U of fusion activity is defined as 1  $\mu$ mol *p*-nitrophenol developed per min and  $\mu$ g *pep4 $\Delta$*  vacuoles.

### Pho8 reporter assay

Reactions (200  $\mu$ l) contained 5  $\mu$ g vacuoles, 1 $\times$  fusion reaction salts (as above), 0.1% Triton X-100, and 30  $\mu$ g/ml proteinase K, in PS buffer. After 15 min at 30°C, enzymatic activity was quenched with the addition of 1 mM PMSF, and fusion reaction developer solution was added, followed by quenching with glycine, pH 11.5 (Haas, 1995). Pho8 activity was measured spectrophotometrically, as for the vacuole fusion assay.

### Online supplemental material

Online supplemental materials, including plasmid and yeast strain construction, the Vps41 purification in Fig. 6 B, Figs. S1–S4, and Table S1, are available at <http://www.jcb.org/cgi/content/full/jcb.200407141/DC1>.

We thank all members of the Ungermann lab for support, especially Lars Dietrich for many thoughtful ideas and discussions, Christine Boedinghaus, Haitong Hou, and Jan Rohde for sharing observations and reagents, and Gabriela Müller and Nadine Decker for expert technical assistance. David Goldfarb (University of Rochester, Rochester, NY), Ed Hurt (University of Heidelberg, Heidelberg, Germany), Michael Knop (EMBL, Heidelberg, Heidelberg, Germany), Sean Munro (MRC, Cambridge, UK), Aki Nakano (Molecular Membrane Biology Laboratory, RIKEN, Saitama, Japan), Janet Shaw (University of Utah, Salt Lake City, UT), Tom Stevens (University of Oregon, Eugene, OR), and Bill Wickner kindly shared plasmids, yeasts, and serum.

This work was supported by a grant of the DFG, the SFB638, the EMBO Young Investigator Programme, the Fonds der Chemischen Industrie (C. Ungermann), and a pre-doctoral fellowship from the National Science Foundation NSFGRFP (to T.J. LaGrassa).

Submitted: 22 July 2004

Accepted: 3 December 2004

## References

- Boedinghaus, C., A.J. Merz, R. Laage, and C. Ungermann. 2002. A cycle of Vam7p release from and PtdIns 3-P-dependent rebinding to the yeast vacuole is required for homotypic vacuole fusion. *J. Cell Biol.* 157:79–90.
- Bonangelino, C.J., N.L. Catlett, and L.S. Weisman. 1997. Vac7p, a novel vacuolar protein, is required for normal vacuole inheritance and morphology. *Mol. Cell. Biol.* 17:6847–6858.
- Bonangelino, C.J., E.M. Chavez, and J.S. Bonifacino. 2002a. Genomic screen for vacuolar protein sorting genes in *Saccharomyces cerevisiae*. *Mol. Cell. Biol.* 13:2486–2501.
- Bonangelino, C.J., J.J. Nau, J.E. Duex, M. Brinkman, A.E. Wurmser, J.D. Gary, S.D. Emr, and L.S. Weisman. 2002b. Osmotic stress-induced increase of phosphatidylinositol 3,5-bisphosphate requires Vac14p, an activator of the lipid kinase Fab1p. *J. Cell Biol.* 156:1015–1028.
- Bone, N., J.B. Millar, T. Toda, and J. Armstrong. 1998. Regulated vacuole fusion and fission in *Schizosaccharomyces pombe*: an osmotic response dependent on MAP kinases. *Curr. Biol.* 8:135–144.
- Bonifacino, J.S., and B.S. Glick. 2004. The mechanisms of vesicle budding and fusion. *Cell.* 116:153–166.
- Brachmann, C.B., A. Davies, G.J. Cost, E. Caputo, J. Li, P. Hieter, and J.D. Boeke. 1998. Designer deletion strains derived from *Saccharomyces cerevisiae* S288C: a useful set of strains and plasmids for PCR-mediated gene disruption and other applications. *Yeast.* 14:115–132.

- Burd, C.G., M. Babst, and S.D. Emr. 1998. Novel pathways, membrane coats and PI kinase regulation in yeast lysosomal trafficking. *Semin. Cell Dev. Biol.* 9:527–533.
- Catlett, N.L., and L.S. Weisman. 1998. The terminal tail region of a yeast myosin-V mediates its attachment to vacuole membranes and sites of polarized growth. *Proc. Natl. Acad. Sci. USA.* 95:14799–14804.
- Colanzi, A., C. Suetterlin, and V. Malhotra. 2003. Cell-cycle-specific Golgi fragmentation: how and why? *Curr. Opin. Cell Biol.* 15:462–467.
- Conibear, E., and T.H. Stevens. 2002. Studying yeast vacuoles. *Methods Enzymol.* 351:408–432.
- Darsow, T., D.J. Katzmann, C.R. Cowles, and S.D. Emr. 2001. Vps41p function in the alkaline phosphatase pathway requires homo-oligomerization and interaction with AP-3 through two distinct domains. *Mol. Biol. Cell.* 12:37–51.
- Dove, S.K., F.T. Cooke, M.R. Douglas, L.G. Sayers, P.J. Parker, and R.H. Michell. 1997. Osmotic stress activates phosphatidylinositol-3,5-bisphosphate synthesis. *Nature.* 390:187–192.
- Dujon, B. 1998. European Functional Analysis Network (EUROFAN) and the functional analysis of the *Saccharomyces cerevisiae* genome. *Electrophoresis.* 19:617–624.
- Eitzen, G., E. Will, D. Gallwitz, A. Haas, and W. Wickner. 2000. Sequential action of two GTPases to promote vacuole docking and fusion. *EMBO J.* 19:6713–6720.
- Fischer von Mollard, G., and T.H. Stevens. 1999. The *Saccharomyces cerevisiae* v-SNARE Vti1p is required for multiple membrane transport pathways to the vacuole. *Mol. Biol. Cell.* 10:1719–1732.
- Gomes de Mesquita, D.S., H.B. van den Hazel, J. Bouwman, and C.L. Woldringh. 1996. Characterization of new vacuolar segregation mutants, isolated by screening for loss of proteinase B self-activation. *Eur. J. Cell Biol.* 71:237–247.
- Gross, S.D., and R.A. Anderson. 1998. Casein kinase I: spatial organization and positioning of a multifunctional protein kinase family. *Cell. Signal.* 10:699–711.
- Haas, A. 1995. A quantitative assay to measure homotypic vacuole fusion in vitro. *Methods Cell Sci.* 17:283–294.
- Haas, A., D. Scheglmann, T. Lazar, D. Gallwitz, and W. Wickner. 1995. The GTPase Ypt7p of *Saccharomyces cerevisiae* is required on both partner vacuoles for the homotypic fusion step of vacuole inheritance. *EMBO J.* 14:5258–5270.
- Jahn, R., T. Lang, and T.C. Südhof. 2003. Membrane fusion. *Cell.* 112:519–533.
- Lowe, M., C. Rabouille, N. Nakamura, R. Watson, M. Jackman, E. Jamsa, D. Rahman, D.J. Pappin, and G. Warren. 1998. Cdc2 kinase directly phosphorylates the cis-Golgi matrix protein GM130 and is required for Golgi fragmentation in mitosis. *Cell.* 94:783–793.
- Mager, W.H., and M. Siderius. 2002. Novel insights into the osmotic stress response in yeast. *FEMS Yeast Res.* 2:251–257.
- Mayer, A., and W. Wickner. 1997. Docking of yeast vacuoles is catalyzed by the Ras-like GTPase Ypt7p after symmetric priming by Sec18p (NSF). *J. Cell Biol.* 136:307–317.
- Mayer, A., W. Wickner, and A. Haas. 1996. Sec18p (NSF)-driven release of Sec17p (alpha-SNAP) can precede docking and fusion of yeast vacuoles. *Cell.* 85:83–94.
- Mellman, I., and G. Warren. 2000. The road taken: past and future foundations of membrane traffic. *Cell.* 100:99–112.
- Müller, O., M.J. Bayer, C. Peters, J.S. Andersen, M. Mann, and A. Mayer. 2002. The Vtc proteins in vacuole fusion: coupling NSF activity to V(0) trans-complex formation. *EMBO J.* 21:259–269.
- Mullins, C., and J.S. Bonifacio. 2001. The molecular machinery for lysosome biogenesis. *Bioessays.* 23:333–343.
- Murakami, A., K. Kimura, and A. Nakano. 1999. The inactive form of a yeast casein kinase I suppresses the secretory defect of the sec12 mutant. Implication of negative regulation by the Hrr25 kinase in the vesicle budding from the endoplasmic reticulum. *J. Biol. Chem.* 274:3804–3810.
- Nass, R., and R. Rao. 1999. The yeast endosomal Na<sup>+</sup>/H<sup>+</sup> exchanger, Nhx1, confers osmotolerance following acute hypertonic shock. *Microbiol.* 145:3221–3228.
- Pan, X., and D.S. Goldfarb. 1998. YEB3/VAC8 encodes a myristylated armadillo protein of the *Saccharomyces cerevisiae* vacuolar membrane that functions in vacuole fusion and inheritance. *J. Cell Sci.* 111:2137–2147.
- Panek, H.R., J.D. Stepp, H.M. Engle, K.M. Marks, P.K. Tan, S.K. Lemmon, and L.C. Robinson. 1997. Suppressors of YCK-encoded yeast casein kinase I deficiency define the four subunits of a novel clathrin AP-like complex. *EMBO J.* 16:4194–4204.
- Peterson, M.R., and S.D. Emr. 2001. The class c vps complex functions at multiple stages of the vacuolar transport pathway. *Traffic.* 2:476–486.
- Piper, R.C., N.J. Bryant, and T.H. Stevens. 1997. The membrane protein alkaline phosphatase is delivered to the vacuole by a route that is distinct from the VPS-dependent pathway. *J. Cell Biol.* 138:531–545.
- Price, A., D. Seals, W. Wickner, and C. Ungermann. 2000. The docking stage of yeast vacuole fusion requires the transfer of proteins from a cis-SNARE complex to a Rab/Ypt protein. *J. Cell Biol.* 148:1231–1238.
- Raymond, C.K., P.J. O'Hara, G. Eichinger, J.H. Rothman, and T.H. Stevens. 1990. Molecular analysis of the yeast VPS3 gene and the role of its product in vacuolar protein sorting and vacuolar segregation during the cell cycle. *J. Cell Biol.* 111:877–892.
- Rehling, P., T. Darsow, D.J. Katzmann, and S.D. Emr. 1999. Formation of AP-3 transport intermediates requires Vps41 function. *Nat. Cell Biol.* 1:346–353.
- Rieder, S.E., and S.D. Emr. 1997. A novel RING finger protein complex essential for a late step in protein transport to the yeast vacuole. *Mol. Biol. Cell.* 8:2307–2327.
- Sato, T.K., P. Rehling, M.R. Peterson, and S.D. Emr. 2000. Class C Vps protein complex regulates vacuolar SNARE pairing and is required for vesicle docking/fusion. *Mol. Cell.* 6:661–671.
- Seals, D.F., G. Eitzen, N. Margolis, W.T. Wickner, and A. Price. 2000. A Ypt/Rab effector complex containing the Sec1 homolog Vps33p is required for homotypic vacuole fusion. *Proc. Natl. Acad. Sci. USA.* 97:9402–9407.
- Seeley, E.S., M. Kato, N. Margolis, W. Wickner, and G. Eitzen. 2002. Genomic analysis of homotypic vacuole fusion. *Mol. Biol. Cell.* 13:782–794.
- Shorter, J., and G. Warren. 2002. Golgi architecture and inheritance. *Annu. Rev. Cell Dev. Biol.* 18:379–420.
- Srivastava, A., C.A. Woolford, and E.W. Jones. 2000. Pep3p/Pep5p complex: a putative docking factor at multiple steps of vesicular transport to the vacuole of *Saccharomyces cerevisiae*. *Genetics.* 156:105–122.
- Sun, B., L. Chen, W. Cao, A.F. Roth, and N.G. Davis. 2004. The yeast casein kinase Yck3p is palmitoylated, then sorted to the vacuolar membrane with AP-3-dependent recognition of a YXX{Phi} adaptin sorting signal. *Mol. Biol. Cell.* 15:1397–1406.
- Tang, F., E.J. Kauffman, J.L. Novak, J.J. Nau, N.L. Catlett, and L.S. Weisman. 2003. Regulated degradation of a class V myosin receptor directs movement of the yeast vacuole. *Nature.* 422:87–92.
- Thorngren, N., K.M. Collins, R.A. Fratti, W. Wickner, and A.J. Merz. 2004. A soluble SNARE drives rapid docking, bypassing ATP and Sec17/18p for vacuole fusion. *EMBO J.* 23:2765–2776.
- Veit, M., R. Laage, L. Dietrich, L. Wang, and C. Ungermann. 2001. Vac8p release from the SNARE complex and its palmitoylation are coupled and essential for vacuole fusion. *EMBO J.* 20:3145–3155.
- Vida, T.A., and S.D. Emr. 1995. A new vital stain for visualizing vacuolar membrane dynamics and endocytosis in yeast. *J. Cell Biol.* 128:779–792.
- Wada, Y., Y. Ohsumi, and Y. Anraku. 1992. Genes for directing vacuolar morphogenesis in *Saccharomyces cerevisiae*. I. Isolation and characterization of two classes of vam mutants. *J. Biol. Chem.* 267:18665–18670.
- Wada, Y., N. Nakamura, Y. Ohsumi, and A. Hirata. 1997. Vam3p, a new member of syntaxin related protein, is required for vacuolar assembly in the yeast *Saccharomyces cerevisiae*. *J. Cell Sci.* 110:1299–1306.
- Wang, C.W., P.E. Stromhaug, E.J. Kauffman, L.S. Weisman, and D.J. Klionsky. 2003. Yeast homotypic vacuole fusion requires the Ccz1-Mon1 complex during the tethering/docking stage. *J. Cell Biol.* 163:973–985.
- Wang, L., E.S. Seeley, W. Wickner, and A.J. Merz. 2002. Vacuole fusion at a ring of vertex docking sites leaves membrane fragments within the organelle. *Cell.* 108:357–369.
- Wang, X., M.F. Hoekstra, A.J. DeMaggio, N. Dhillon, A. Vancura, J. Kuret, G.C. Johnston, and R.A. Singer. 1996. Prenylated isoforms of yeast casein kinase I, including the novel Yck3p, suppress the gcs1 blockage of cell proliferation from stationary phase. *Mol. Cell Biol.* 16:5375–5385.
- Wang, Y.X., H. Zhao, T.M. Harding, D.S. Gomes de Mesquita, C.L. Woldringh, D.J. Klionsky, A.L. Munn, and L.S. Weisman. 1996. Multiple classes of yeast mutants are defective in vacuole partitioning yet target vacuole proteins correctly. *Mol. Biol. Cell.* 7:1375–1389.
- Wang, Y.X., N.L. Catlett, and L.S. Weisman. 1998. Vac8p, a vacuolar protein with armadillo repeats, functions in both vacuole inheritance and protein targeting from the cytoplasm to vacuole. *J. Cell Biol.* 140:1063–1074.
- Weisman, L.S. 2003. Yeast vacuole inheritance and dynamics. *Annu. Rev. Genet.* 37:435–460.
- Whyte, J.R., and S. Munro. 2002. Vesicle tethering complexes in membrane traffic. *J. Cell Sci.* 115:2627–2637.
- Wickner, W. 2002. Yeast vacuoles and membrane fusion pathways. *EMBO J.* 21:1241–1247.
- Wurmser, A.E., T.K. Sato, and S.D. Emr. 2000. New component of the vacuolar class C-Vps complex couples nucleotide exchange on the Ypt7 GTPase to SNARE-dependent docking and fusion. *J. Cell Biol.* 151:551–562.
- Zerial, M., and H. McBride. 2001. Rab proteins as membrane organizers. *Nat. Rev. Mol. Cell Biol.* 2:107–117.